Much of Zero Emissions Commitment Occurs Before Reaching Net Zero Emissions

Charles D. Koven[1*], Benjamin M. Sanderson[2], Abigail L. S. Swann[3]

1. Climate and Ecosystem Sciences Division, Lawrence Berkeley National Laboratory, Berkeley, California, USA
2. Centre for International Climate and Environmental Research (CICERO), Oslo, Norway
3. Department of Atmospheric Science and Department of Biology, University of Washington, Seattle, WA, USA

***Email:** cdkoven@lbl.gov

Abstract

We explore the response of the Earth's climate and carbon system to an idealized sequential addition and removal of CO_2 to the atmosphere, following a symmetric and continuous emissions pathway, in contrast to the discontinuous emissions pathways that have largely informed our understanding of the climate response to net-zero and net-negative emissions to date. We find, using both an Earth System Model and an ensemble of simple climate model realizations, that warming during the emissions reduction and negative emissions phases is defined by a combination of a proportionality of warming to cumulative emissions characterized by the transient climate response to emissions (TCRE), and a deviation from that proportionality that is governed by the zero emissions commitment (ZEC). About half of the ZEC is realized before reaching zero emissions, and the ZEC thus also controls the timing between peak cumulative CO_2 emissions and peak temperature, such that peak temperature may occur before peak cumulative emissions if ZEC is negative, underscoring the importance of ZEC in climate policies aimed to limit peak warming. Thus we argue that ZEC is best defined as the committed warming relative to the expected TCRE proportionality, rather than the additional committed warming that will occur after reaching net zero CO_2 emissions. Once established, the combined TCRE and ZEC relationship holds almost to complete removal of prior cumulative CO_2 emissions. As cumulative CO_2 emissions approach zero through negative CO_2 emissions, CO_2 concentrations drop below preindustrial values, while residual long-term climate change continues, governed by multicentennial dynamical processes.

Significance Statement

We use climate models to explore both the amount of global warming and the relative timing between warming and carbon dioxide emissions, under an idealized scenario where carbon dioxide emissions gradually cease and then reverse, such that the timing and amount of carbon dioxide removals is exactly the reverse of prior emissions. We find that a metric of long-term committed warming begins to occur soon after emission rates peak, and controls the timing of when temperatures begin to cool relative to when net-zero carbon dioxide emissions occur. Overall, we find that global warming is proportional to cumulative carbon dioxide emissions plus the committed warming metric as we start to reduce and eventually reverse emissions.

Introduction

Current climate policy is predicated on the idea that the magnitude of global warming is proportional to cumulative emissions of carbon dioxide (1, 2). This relationship emerges from complex interactions between the physical and biogeochemical aspects of the Earth system, and has been consistent across all coupled carbon-climate models under scenarios of positive CO_2 emissions (3, 4). The simplicity and path independence of the relationship allow the creation of a remaining carbon budget consistent with a specific warming level. However, the path independence of the relationship between warming and cumulative CO_2 emissions, known as the Transient Climate Response to Emissions (TCRE), is only approximate – for example it is possible that some remaining CO_2-driven temperature change will occur even after emissions cease, and this deviation from the path independence of the TCRE approximation can be quantified as the Zero Emission Commitment (ZEC) (5–7), which is used alongside the TCRE in constructing a remaining carbon budget for climate stabilization for policy applications (8).

The modeled proportionality of warming to cumulative emissions, despite emerging from complex and at least partially coincidental interactions (9–11), holds to a remarkably high amount of cumulative emissions (12, 13). Likewise, under negative CO_2 emissions, the proportionality of warming to cumulative CO_2 emissions still holds as cumulative emissions decrease, subject to an asymmetry that is governed by the ZEC (13) in both idealized (14) and scenario-driven (13) experiments for overshoots up to ~300 Pg C. Thus, a hypothetical framework for highly mitigated scenarios, that long-term warming equals the sum of cumulative emissions times TCRE plus a committed ZEC value, may hold from net zero to net negative emissions. While the expected time lag between CO_2 emissions and CO_2-driven warming is only about a decade (15), the controls of that lag remain insufficiently quantified. The idealized experiments used to quantify TCRE and ZEC, where TCRE is the warming during the exponential CO_2 concentration growth phase (16) and ZEC is the subsequent warming after emissions instantaneously go to zero (17) do not allow assessment of when ZEC may occur as emissions decrease on the path to net zero or net negative CO_2 emissions.

It is also not clear how far the relationship between warming, cumulative emissions and ZEC described above would hold under negative emissions. Thus, here we ask whether temperature remains proportional to cumulative emissions, plus a ZEC value, as far as to the net removal of all anthropogenic CO_2 emissions in pursuit of restoration of the climate system to a preindustrial-like state, which we term a restoration scenario. Previous work on the reversibility of climate change under declining CO_2 has used time-reversed CO_2 concentration scenarios, with either idealized (18–21) or scenario-driven (22, 23) experiments. These experiments are critical in showing asymmetries in the climate and carbon cycle with respect to changing CO_2 concentrations, e.g., that there is a substantial lag between global temperature change and CO_2 concentrations after the transition from positive to negative emissions(24). While, in general,

concentration-driven experiments can be used to infer emissions and thus frame climate outcomes in terms of compatible emissions, the abrupt reversal from increasing to declining CO_2 concentrations in these scenarios requires a highly discontinuous emissions timeseries, instantly changing ~50 Pg C/yr from large positive to large negative values (fig. S1a). Because the inertia of the Earth system acts like a low-pass filter, it is possible that this abrupt and very large change in emissions, which also holds for pulse CO_2 emission or removal experiments (15, 25), pushes the path independence of the TCRE to the point where it may no longer hold on shorter timescales. For example, in idealized 1%/yr reversal experiments, the proportionality of warming to cumulative emissions does not generally hold, as global temperatures are warmer for a given level of emission during the negative emissions period than during the positive emissions period(19), which we also find for the CMIP6 CDRMIP ensemble mean (fig. S1b). In scenario-based overshoot projections, the transition from positive to negative emissions takes decades (fig. S2), thus such large abrupt transitions in emissions are unlikely to occur.

We thus design and perform an idealized emission-driven carbon dioxide removal (CDR) experiment with the following three goals: we seek first to avoid sharp discontinuities in emissions, so as not to break the path-independence of the TCRE relationship or the timing of ZEC emergence due to any such discontinuities, second to have roughly exponential ramp-up of emissions early in the scenario to match the shape of historical emissions, and third to keep emissions symmetric in time before and after net zero to explore asymmetries in carbon fluxes and climate responses with respect to emissions. A simple experimental design that satisfies all of these criteria is to let cumulative CO_2 emissions follow a Gaussian curve in time, and thus let annual emissions follow the first derivative of a Gaussian. We force both the Community Earth System Model, version 2 (CESM2) (26) and a simple climate model FaIR 1.3 (27, 28) under such a scenario, with cumulative emissions reaching a maximum of 1000 Pg C after 150 years of simulation, and returning to zero after 300 years (figs 1a-b). This climate restoration experiment then allows us to ask several related questions: (1) how would the Earth system respond to the removal of all previously-emitted CO_2, (2) what are the lags and asymmetries of the transient response of climate and carbon cycle dynamics to a symmetric shift from positive to negative CO_2 emissions around the point of the emissions reversal, and (3) how does the ZEC impact the relative timing between peak cumulative emission and peak warming?

Results

Carbon fluxes between the atmosphere and both the terrestrial and ocean systems follow emissions, with both the land and ocean sinks changing sign to become sources after the reversal from positive to negative CO_2 emissions (figure 1a). Lags, as quantified by the interval of maximum lagged correlation, between emissions and carbon sinks are longer (20 years) for the terrestrial carbon cycle than the ocean (11 years), with the combined land and ocean sink in between (16 years). At the point of reaching maximum cumulative emissions, the lag in land and

ocean sinks with respect to emissions means that the sinks are still positive, and thus that the atmospheric CO_2 concentration is already declining as emissions trend towards zero. Thus peak concentrations are reached before zero emissions, and more generally, this means that the rate of change of atmospheric CO_2 leads emissions, here by 13 years. This result—that atmospheric CO_2 change leads emissions by approximately the same timescale that sinks lag emissions—follows from the general trigonometric identity for the phase of summed functions if both emissions and sinks follow sinusoidal curves (SI text). The lead of atmospheric growth rate relative to emissions is consistent with that between diagnosed fossil fuel emissions in SSP scenarios that reach net zero as reported by ref (29) where, e.g. in the SSP5-3.4-overshoot scenario, CO_2 concentrations peak in 2062, while net fossil CO_2 emissions reach zero between 2068-2078, depending on the Earth system model.

Integrated CO_2 fluxes (figure 1b) show asymmetries in the accumulation of carbon during the positive and negative emissions periods. In particular, at the point of reaching zero cumulative emissions near the end of the experiment, the cumulative atmospheric sink is negative, i.e. CO_2 concentrations are below the preindustrial value, reaching a minimum value of 258 ppm, versus an initial value of 289 ppm and maximum value of 506 ppm (fig. 2a). Land carbon at the end is also slightly below the preindustrial value, with the excess carbon in the ocean. Looking further at the partitioning of carbon within the land and ocean systems (figs.1c-d) shows that the excess carbon is at depth, with shallow ocean DIC anomalies following closely the atmospheric timeseries and lag increasing with depth. Thus, even though the ocean shows a shorter lag than the land with respect to flux correlations against emissions, the difference at the end of the simulations is greater. The positive emissions pulse is able to propagate more fully into the deep ocean than the negative emissions pulse, leading to the positive ocean carbon difference at the end of the simulation. On land, there is likewise a difference in lags between vegetation and soil carbon (fig 1d), as well as an asymmetric response in that both lose carbon after peak emissions more rapidly than they gained carbon prior to the peak, which follows from the asymmetry of atmospheric CO_2 timeseries. Zonal-mean land carbon changes (fig. S3) show a stronger latitudinal dependence to the timing of soil carbon than vegetation carbon responses.

The phasing between the physical climate and CO_2 emissions (fig. 2a) shows that global mean surface temperature anomalies actually lead the CO_2 emissions, with a maximum correlation at lead of 5 years. This happens because atmospheric CO_2 concentrations lead emissions by more than the physical climate lags CO_2 concentrations. This result is consistent with, though stronger than, the current policy framework that says that reaching zero emissions will lead to effectively immediate stabilization of CO_2-driven global warming. Here, the suggestion from CESM2 is that CO_2-driven temperature stabilization may actually occur before reaching net-zero CO_2 emissions. Global precipitation anomalies lag both temperature and CO_2 emissions (fig. 2a). CESM2 has a particularly strongly negative ZEC value of -0.34C, which may be manifesting fairly soon after the emissions peak and decline, as was also found in the comparison between

ZEC diagnosed from instantaneous transition to net-zero versus gaussian emissions (17). Thus it is possible that the relative timing between achieving net-zero CO_2 emissions and temperature stabilization is itself dependent on ZEC.

As described above, the hypothesis here is that long-term warming after achieving net negative emissions equals the sum of cumulative emissions (CE) times TCRE, plus a committed ZEC value (13). Thus we expect that CESM2, which has a strongly negative ZEC_{90} value of -0.34C (17), will have an equally negative overshoot asymmetry, i.e. with colder temperatures for a given amount of cumulative emissions after reaching net-negative emission than before. This is roughly what we find (figure 2b). For most of the positive emissions period, temperature follows the expected proportionality given the previously-reported value of TCRE for the model of 2.13 degree/Eg C (16), however, the model falls off the $\Delta T = TCRE * CE$ line after emission rates begin to decline from their maximum values, and relaxes towards a line representing $\Delta T = TCRE * CE + ZEC$, and then follows that line from the point of reaching net negative emissions through almost all the way until net cumulative CO_2 emissions are back to zero. After that point, global mean surface temperatures begin to rise again, even though cumulative emissions continue to fall until reaching zero.

The increase in temperatures at the end of the CESM2 simulation, when cumulative emissions are approaching zero, shows a distinct regional pattern, with maximum cooling in mid-high northern latitudes at years 200-250, followed by a reversal to warming afterwards (fig. S4a). The spatial pattern and timing relative to the reversal of CO_2 emissions is consistent with that observed in CESM2-WACCM for the SPP5-3.4-overshoot scenario, due to a re-strengthening of AMOC after its transient weakening with warming (13). A similar dynamic occurs here, but even more strongly, with AMOC strengthening well beyond its preindustrial value in response to the negative emissions (fig. S4b). Thus the long-timescale warming reflects the interactions between the direct forced temperature changes from CO_2 with the indirect response of AMOC and associated heat transport.

Any single Earth system model, such as CESM2, represents only one estimate of the complex dynamics of the Earth system. To understand more generally how the carbon-climate sensitivity metrics TCRE and ZEC govern the transient dynamics of the Earth system to an emissions reversal, we use the Finite Amplitude Impulse Response (FaIR) simple climate model (27) to perform a perturbed parameter ensemble (PPE) of simulations using the same emissions forcing pathway. We find that the 10-90th percentile range of global mean surface temperature variation in response to the forcing broadly follows the pattern of the CESM2 simulation (fig 3a). Differences between CESM2 and the FaIR ensemble are strongest at the end of the experiment, when CESM2 shows a pronounced warming due to AMOC restrengthening (a process not included in FaIR), while the FaIR simulations show a range of responses, from cooling to warming. Figure 3(b-g) shows scatterplots of TCRE and ZEC_{100} for each ensemble against key

climate response variables. Peak warming is highly correlated with TCRE (fig. 3b-c), the lag between peak emissions and peak warming is governed primarily by ZEC (fig. 3d-e), and a weak control by ZEC on the temperature change at the end of the simulation (fig. 3f-g). We find that using both TCRE and ZEC in a multivariate linear prediction of end of simulation warming provides no additional predictive skill over using ZEC alone (not shown).

We show where in the forcing trajectory different combinations of sensitivity metrics (i.e. TCRE and ZEC at different timescales) have the strongest predictive power by plotting temperature versus cumulative emissions for each of the FaIR PPE simulations and noting where the minimum spread across the ensemble occurs (fig. 4). Normalizing the warming of each FaIR ensemble member by that ensemble's TCRE (fig. 4a) shows a minimum ensemble spread (marked by vertical dashed lines) midway through the positive emissions phase of the simulation, with spread increasing as cumulative emissions approach their maximum. Normalizing warming by TCRE plus half of the ZEC_{50} for each ensemble member (fig. 4b) moves the minimum ensemble spread to the point of maximum cumulative emissions, i.e. half of the ZEC has already manifested in these simulations at the point of reaching zero emissions. Normalizing by TCRE plus either ZEC_{50} (fig. 4c) or ZEC_{100} (fig. 4d) shifts the point of minimum ensemble spread to either the early (fig. 4c) or middle (fig. 4d) of the negative emissions period, showing that the timescale by which ZEC is defined governs where in the negative emissions trajectory that sensitivity is realized.

The experiment here is only one realization from a wide set of possible idealized CO_2 emissions reversibility experiments. Key variables that may affect the carbon and climate response are the total peak emissions and the timescale for emissions growth and reversal. We use FaIR to explore how the dynamics described above may vary in response to these alternate emissions trajectories (fig. 5). We find: (1) that the transient drop in CO_2 concentrations below preindustrial values near the end of the simulation is a robust feature of any symmetric CO_2 emissions reversal (fig. 5b, 5e); (2) that the peak warming amount is roughly insensitive to the timescale of emissions (fig. 5c); (3) that there tends to be a minimum in warming late in the period of net-negative CO_2 emissions, which is followed by a re-emergence of warming after the negative-emissions phase (fig. 5c, 5f); (4) that the lag between peak emissions and peak warming increases with higher peak cumulative emissions (30) (fig 5f); and (5) that the long-term warming after emissions reversal is higher with higher peak cumulative emissions (fig. 5f).

Discussion

The Paris agreement calls for stabilization of the global climate at levels well below two degrees Celsius, and IPCC AR6 assesses that such climate stabilization requires reaching net zero CO_2 emissions (IPCC, 2021). Overshoot scenarios are premised on the idea that we may be unable to avoid surpassing target warming levels, and instead may require large amounts of net-negative

CO_2 emissions to cool and then stabilize the climate system at the agreed warming levels. Significant climate impacts are already evident at the current warming level of 1.1 degrees Celsius. Thus future generations, if they are able to develop the means to generate the large net negative CO_2 emissions required for overshoot, may wish to try to restore the climate system to a preindustrial-like state, rather than stabilize it at some target level of warming well above the preindustrial. While it is not clear whether long-term CDR technologies could ever be deployed at the scale necessary to reach net negative CO_2 emissions (31), particularly at the scale considered here (32, 33), or, even if they could, whether the deleterious effects of these technologies would outweigh their potential benefits (33, 34), it is nonetheless important to understand how the coupled carbon and climate systems would respond to a transient reversal from net positive, through net zero, and to net negative CO_2 emissions in order to translate timelines of mitigation ambitions into expected climate damages.

We find that under this restoration scenario the land and ocean carbon sinks follow the trajectories of CO_2 emissions, becoming sources soon after emissions become negative, consistent with the results from overshoot scenarios (13, 35). The relative timing of this transition differs between land and ocean: the ocean responds in CESM2 more rapidly than land in its sink-to-source transition, even though the ocean also shows a greater stock of carbon at the end of the simulation, and thus a longer memory to carbon perturbations, than the land. This reflects that both land and ocean exchange carbon with the atmosphere at multiple timescales (36), for land due to the sequence of live and dead pools that carbon passes through, and for the ocean due to the strong gradient in timescales of carbon response to atmospheric perturbations with depth.

In this scenario, for both CESM2 and FaIR, the relationship between global mean temperature and emissions can roughly be broken into three phases. In the first phase, temperature change is proportional to cumulative emissions, with a proportionality well described by the TCRE (ΔT = TCRE * CE). This phase lasts until roughly the point where emissions rates peak. In the second phase, the influence of the ZEC begins to be felt, as the relationship shifts towards one characterized by ΔT = TCRE * CE + ZEC. This phase begins roughly at the time of peak emissions rates, i.e. well before reaching net zero, and lasts through most of the period of net-negative CO_2 emissions and almost towards the point where cumulative emissions reach zero. Because much of the ZEC influence occurs before the time of reaching net zero, its magnitude governs both the timing between peak cumulative emissions and peak temperature as well as the peak warming that is reached. The third phase is characterized by long-term climate and carbon responses that govern the committed temperature change even after all anthropogenic carbon is removed from the system.

The relative lag between temperature change and emissions of CO_2, as well as the remaining temperature change after reaching net zero CO_2 emissions, are of utmost importance to policy

and our ability to keep the climate system below warming targets. Both with CESM2 and FaIR, which between them span the range of model complexity, we find a strong relationship between the ZEC and the lag between peak cumulative emissions and peak temperature, such that if ZEC is negative then peak temperature may actually lead peak cumulative emissions.

ZEC has typically been described as the committed temperature change expected to occur a given period after reaching net zero CO_2 emissions (7, 17). However, because the standard quantification of ZEC is made relative to an instantaneous transition to zero emissions from the same 1% yr^{-1} increasing concentration experiment (7, 17) that is also used to quantify TCRE, that quantification is also consistent with a second distinct definition of ZEC as the committed temperature change relative to expectations from TCRE proportionality at the point of reaching zero CO_2 emissions. This experiment, as well as the Gaussian emissions experiment described in ref. (17), show that the second interpretation is more correct, because the ZEC can become evident before reaching net zero CO_2 emissions when the transition occurs as part of a gradual emissions reduction. Put another way, ZEC can't describe the amount of temperature change that is still to occur after reaching net zero when half, or even all in the case of CESM2, of that temperature change actually occurs before reaching net zero emissions. In less idealized scenarios, the relative timing between peak warming and peak cumulative CO_2 emissions will also be governed by the dynamics non-CO_2 greenhouse gasses, and in particular the relative rates of decline of cooling versus warming short-lived climate pollutants.

The ZEC governs several aspects of the global temperature dynamics in this scenario. First, ZEC governs the asymmetry in the temperature to cumulative emissions relationship between the positive and negative emissions phases. Second, because much of the ZEC occurs before reaching net zero, it affects the magnitude and governs the timing of peak global warming. IPCC AR6 assessed that the best estimate of ZEC is zero, with a likely range of ±0.3C, and low confidence in the sign (24). If the Earth's ZEC is negative, our findings suggest that CO_2-driven climate change may begin to reverse slightly before reaching net zero CO_2 emissions, sooner than the decade-lag that is currently estimated (15, 24), with important implications for policy.

Across all highly-mitigated CO_2 emissions trajectories, there is a consistency in the committed global warming, relative to the TCRE proportionality, upon reaching peak cumulative emissions, that is well quantified by the ZEC at various timescales, and that occurs whether subsequent emissions are net zero or net negative. If large-scale net negative CO_2 emissions are both possible and pursued, we should expect temperatures to follow the same TCRE slope in response to those emissions down almost to the point of zero cumulative CO_2 emissions, underscoring the potential efficacy of net negative CO_2 emissions for restoration of the climate system in the distant future. Lastly, the result that much of the ZEC may occur by the time of reaching net zero emissions underscores the importance of the ZEC metric, even on the short timescales required to reach net zero in order to reach Paris Agreement targets, and that better quantifying ZEC is

crucial to understand both peak CO_2-driven warming and the relative timing between peak warming and peak cumulative CO_2 emissions.

Methods

The annual emissions timeseries *E(t)* [Pg C/yr] for year *t* follows the form of the first derivative of a Gaussian:

$$E(t) = \frac{a\,(b-t)\,e^{\frac{-(b-t)^2}{2c^2}}}{c^2}$$

For the experiment here, we used values for *a (*maximum cumulative emissions) of 1004 Pg C, *b* (year of peak cumulative emissions) of year 150, and *c* (timescale for emissions reversal) of 45. We used a value of *c* 1004 Pg C, rather than 1000 Pg C, because the cumulative emissions evaluated at year 1 is 4 Pg C, thus the total integrated emissions over the period from year 1 to year 150 is 1000 Pg C, and from year 151 to year 300 is -1000 Pg C. After year 300, we set annual emissions to zero Pg C/ yr. Emission fluxes are spread equally over land and ocean of the entire planet. We note that the magnitude of ZEC is itself a function of maximum cumulative emissions (17), so we use the same maximum cumulative emissions here (1000 Pg C) as in the standard ZECMIP experiment.

We use the CESM2 (26), version 2.1.3, in an emissions-driven mode, (compset 'B1850_BPRP') with the default initial conditions for the emissions-driven configuration (year 151 of reference (37)). For the transient simulation, all non-CO_2 aspects of the model were kept at preindustrial values, and CO_2 concentrations were prognostic in response to the specified emissions timeseries. Output fluxes and climate variables were smoothed using an 11-year Savitzky-Golay filter to remove interannual variability.

Simple climate model simulations were conducted with a large perturbed parameter ensemble using the FaIR 1.3 model (27, 28). We use 1000 ensemble members, with model radiative forcing parameters sampled following ref (27), with an extended sampling of model thermal and carbon timescale parameters sampled as detailed in Tables S1-S3, where parameter ranges are informed by a number of studies exploring the emulation of Earth System Models with an impulse response formulation (38–40). Ensemble configurations are filtered according to their ability to reproduce historical global temperature pathways as in ref. (41), leaving 207 filtered ensemble members. For each ensemble member, we calculate the response to the idealised CDR pathways, as well as standard emissions-driven metrics of TCRE (42) and ZEC (17). TCRE is here calculated as the warming in year 70 of a concentration driven simulation (where concentrations increase from pre-industrial levels at 1 percent per year until concentrations are doubled in approximately year 70) divided by compatible emissions (E_{1pct}) derived using an inverse FaIR simulation (27). Zero Emissions Commitment is calculated by running the forward

model with (E_{1pct}) until year 70, with zero emissions thereafter (7). ZEC_{50} and ZEC_{100} are measured as the temperature change between year 70 and years 120 and 170 respectively.

Figures

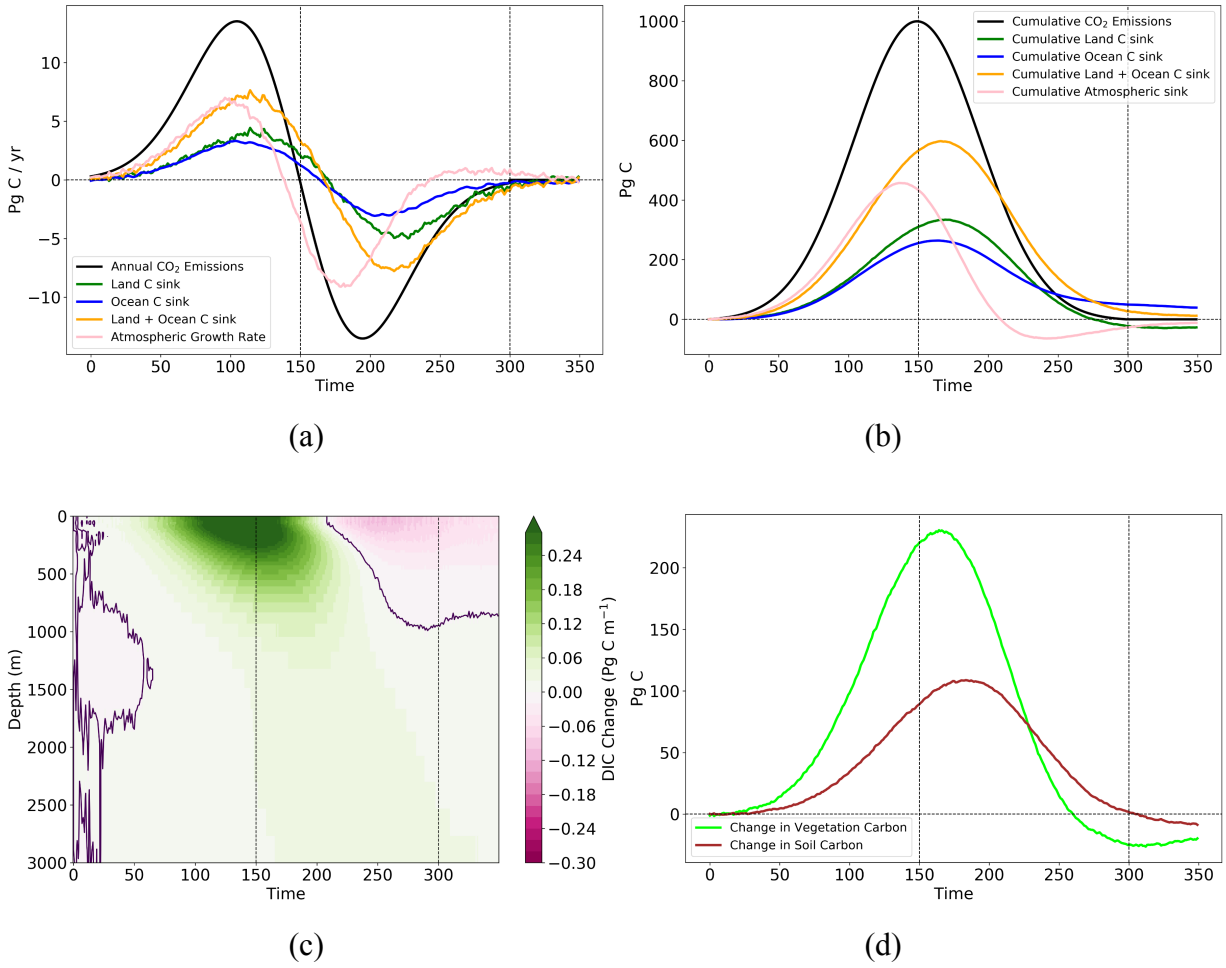

Fig. 1 (a) CO_2 fluxes and (b) integrated CO_2 fluxes in response to the idealized emissions reversal scenario for CESM2. (c) Globally-integrated dissolved inorganic carbon (DIC) stock changes as a function of depth (Pg C/m) in the ocean, and (d) Globally-integrated changes in vegetation and soil (including litter and coarse woody debris) carbon stocks (Pg C) on land. Vertical dashed lines note times of peak cumulative emissions and return to zero cumulative emissions.

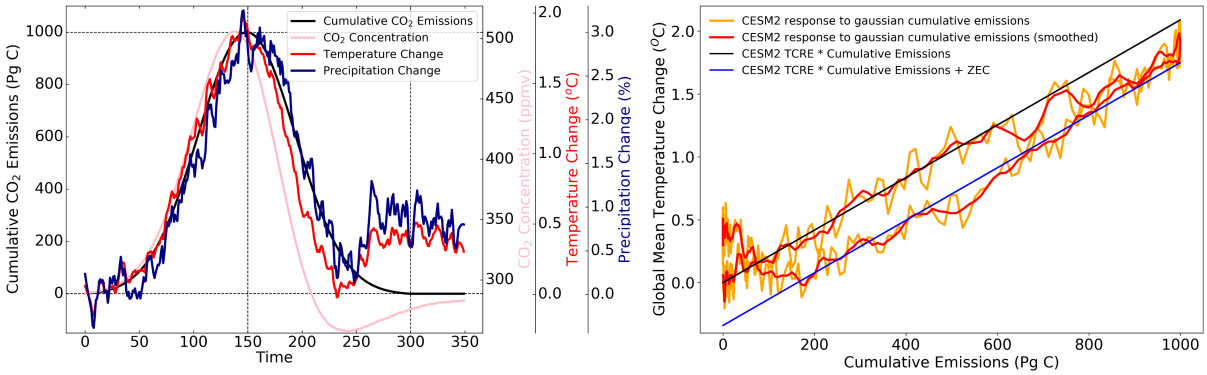

(a) (b)

Fig. 2 (a) Timeseries of relative values of CO_2 emissions, global mean CO_2 concentrations, global mean surface temperature anomaly, and global mean precipitation anomaly under the idealized emissions reversal scenario for CESM2. (b) Global warming as a function of cumulative emissions for the scenario. The slope of the black line is the previously-reported value of transient climate response to cumulative CO_2 emissions (TCRE) for CESM2, and the blue line is offset from the black line by the previously-reported value of the zero emissions commitment (ZEC) for CESM2. Vertical dashed lines in (a) note times of peak cumulative emissions and return to zero cumulative emissions.

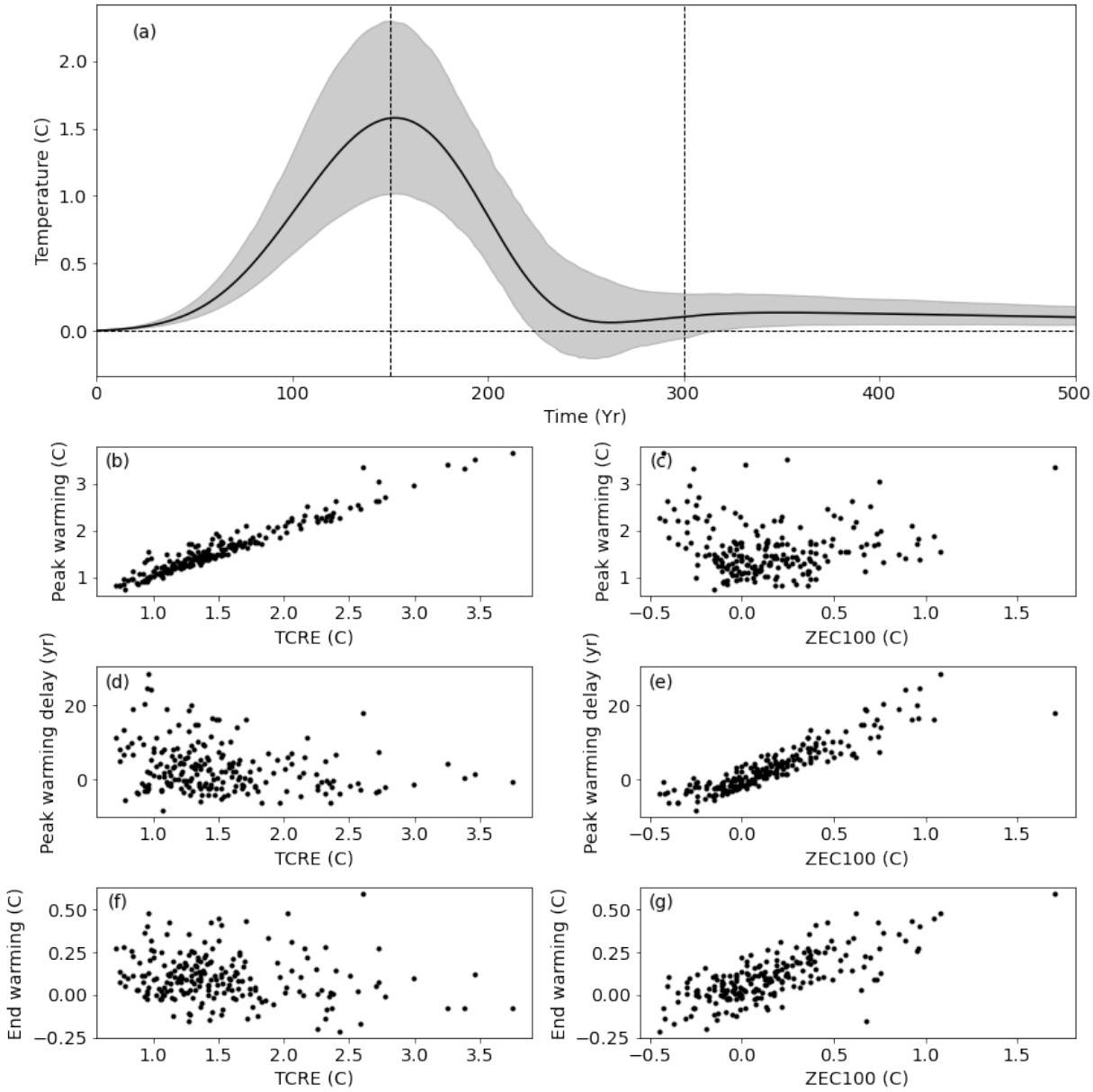

Fig. 3 (a) Range of temperature responses to idealized emissions reversal using an ensemble of FaIR simple climate model realizations. (b-g) Relationship between peak warming, lag of peak temperature to peak warming, and warming at the end of the experiment to the climate sensitivity metrics TCRE and 100-year ZEC (ZEC_{100}), using FaIR simple climate model. Vertical dashed lines in (a) note times of peak cumulative CO_2 emissions and return to zero cumulative emissions.

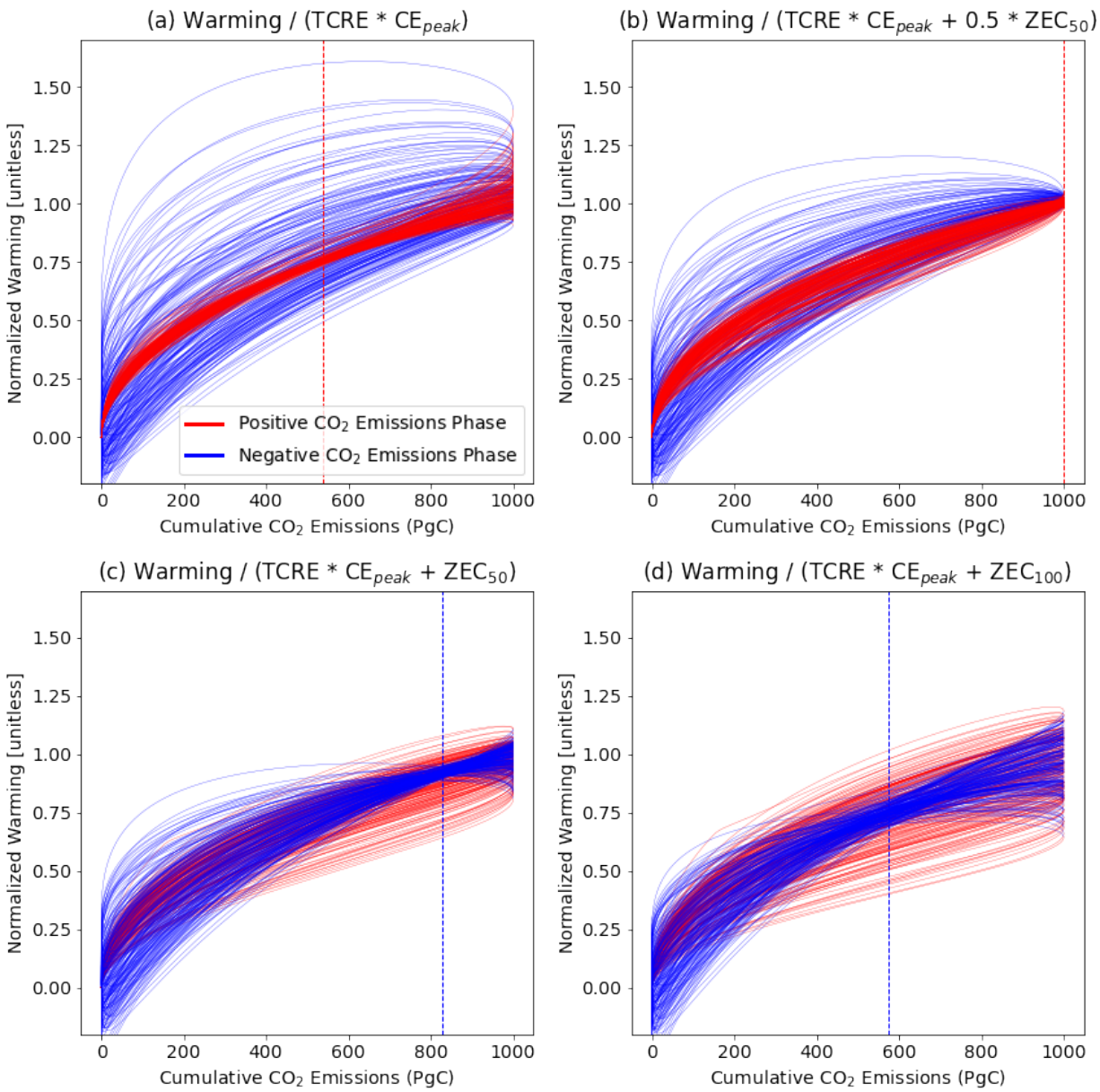

Fig. 4. Temperature vs cumulative CO_2 emissions relationship for the FaIR simple climate model ensemble driven by the idealized emissions reversal scenario. Red curves are for the positive emissions phase (years 0-150) and blue for the negative emissions phase (years 151-300) of the scenario. Panels differ in the normalization of warming for each ensemble member on the y axis, in order to show where along the trajectory each normalization minimizes the spread across the ensemble: (a) warming divided by TCRE * peak cumulative emissions (CE_{peak}, which equals 1000 Pg C for all ensembles); (b) warming divided by TCRE * CE_{peak} + half of the ZEC_{50}; (c) warming divided by TCRE *CE_{peak} + ZEC_{50}; (c) warming divided by TCRE *CE_{peak} + ZEC_{100}. Positive emissions phase curves are foregrounded in panels a-b, negative emissions phase curves are foregrounded in panels c-d. Vertical dashed lines show the cumulative emissions that correspond to minimum ensemble spread in normalized temperature across the ensemble for

each panel, also colored by the emissions phase during which that minimum spread occurs (red=positive, blue=negative).

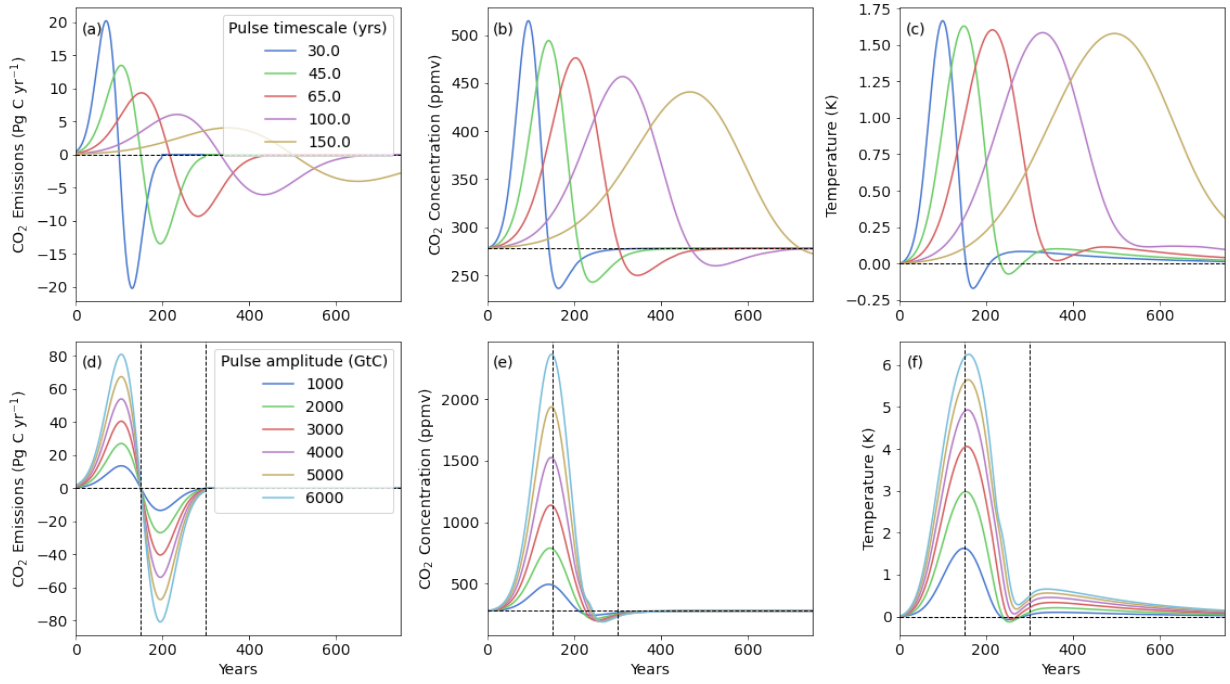

Fig. 5 Sensitivity to timescale and amplitude of forcing (a-c) sensitivity to timescale of carbon reversal in FaIR simple climate model. Reference case (all prior results) uses a 45 year pulse timescale and 1000 Pg C maximum cumulative emissions. Vertical dashed lines in (d-f) note times of peak cumulative emissions and return to zero cumulative emissions.

Data availability

All CESM2 data for the experiment described here will be made available at time of publication. All scripts to generate and analyze climate model output here are available at https://github.com/ckoven/idealized_emissionsdriven_cdr_scenario.

Acknowledgements

CDK acknowledges support by the Director, Office of Science, Office of Biological and Environmental Research of the US Department of Energy under contract DE-AC02-05CH11231 through the Regional and Global Model Analysis Program (RUBISCO SFA). BS acknowledges support by H2020 programs ESM2025 (grant agreement no. 101003536) and 4C (GA 821003). ALSS acknowledges support from DOE BER RGMA award DE-SC0021209 to the University of Washington. We acknowledge the World Climate Research Programme, which, through its Working Group on Coupled Modelling, coordinated and promoted CMIP6. We thank the climate

modeling groups for producing and making available their model output, the Earth System Grid Federation (ESGF) for archiving the data and providing access, and the multiple funding agencies who support CMIP6 and ESGF. Computing resources (https://doi.org/10.5065/D6RX99HX) were provided by the Climate Simulation Laboratory at NCAR's Computational and Information Systems Laboratory, sponsored by the National Science Foundation and other agencies.

References

1. IPCC Working Group I, *Climate Change 2013 - The Physical Science Basis: Summary for Policymakers* (2013).

2. Ipcc, "Summary for Policymakers. In: Climate Change 2021: The Physical Science Basis. Contribution of Working Group I to the Sixth Assessment Report of the Intergovernmental Panel on Climate Change," V. Masson-Delmotte, *et al.*, Eds. (2021).

3. M. R. Allen, *et al.*, Warming caused by cumulative carbon emissions towards the trillionth tonne. *Nature* **458**, 1163–1166 (2009).

4. H. D. Matthews, N. P. Gillett, P. A. Stott, K. Zickfeld, The proportionality of global warming to cumulative carbon emissions. *Nature* **459**, 829–832 (2009).

5. H. D. Matthews, K. Caldeira, Stabilizing climate requires near-zero emissions. *Geophys. Res. Lett.* **35** (2008).

6. S. Solomon, G.-K. Plattner, R. Knutti, P. Friedlingstein, Irreversible climate change due to carbon dioxide emissions. *Proc. Natl. Acad. Sci. U. S. A.* **106**, 1704–1709 (2009).

7. C. D. Jones, *et al.*, The Zero Emissions Commitment Model Intercomparison Project (ZECMIP) contribution to C4MIP: quantifying committed climate changes following zero carbon emissions. *Geoscientific Model Development* **12**, 4375–4385 (2019).

8. J. Rogelj, P. M. Forster, E. Kriegler, C. J. Smith, R. Séférian, Estimating and tracking the remaining carbon budget for stringent climate targets. *Nature* **571**, 335–342 (2019).

9. M. R. Raupach, The exponential eigenmodes of the carbon-climate system, and their implications for ratios of responses to forcings. *Earth Syst. Dynam.* **4**, 31–49 (2013).

10. P. Goodwin, R. G. Williams, A. Ridgwell, Sensitivity of climate to cumulative carbon emissions due to compensation of ocean heat and carbon uptake. *Nat. Geosci.* **8**, 29–34 (2015).

11. A. H. MacDougall, P. Friedlingstein, The origin and limits of the near proportionality between climate warming and cumulative CO2 emissions. *J. Clim.* **28**, 4217–4230 (2015).

12. K. B. Tokarska, N. P. Gillett, A. J. Weaver, V. K. Arora, M. Eby, The climate response to five trillion tonnes of carbon. *Nat. Clim. Chang.* **6**, 851–855 (2016).

13. C. D. Koven, *et al.*, Multi-century dynamics of the climate and carbon cycle under both high and net negative emissions scenarios. *Earth System Dynamics* **13**, 885–909 (2022).

14. K. B. Tokarska, K. Zickfeld, J. Rogelj, Path independence of carbon budgets when meeting a stringent global mean temperature target after an overshoot. *Earths Future* **7**, 1283–1295 (2019).

15. K. L. Ricke, K. Caldeira, Maximum warming occurs about one decade after a carbon dioxide emission. *Environ. Res. Lett.* **9**, 124002 (2014).

16. V. K. Arora, *et al.*, Carbon–concentration and carbon–climate feedbacks in CMIP6 models and their comparison to CMIP5 models. *Biogeosciences* **17**, 4173–4222 (2020).

17. A. H. MacDougall, *et al.*, Is there warming in the pipeline? A multi-model analysis of the Zero Emissions Commitment from CO 2. *Biogeosciences* **17**, 2987–3016 (2020).

18. O. Boucher, *et al.*, Reversibility in an Earth System model in response to CO2 concentration changes. *Environ. Res. Lett.* **7**, 024013 (2012).

19. K. Zickfeld, A. H. MacDougall, H. Damon Matthews, On the proportionality between global temperature change and cumulative CO2 emissions during periods of net negative CO2 emissions. *Environ. Res. Lett.* **11**, 055006 (2016).

20. T. Ziehn, A. Lenton, R. Law, An assessment of land-based climate and carbon reversibility in the Australian Community Climate and Earth System Simulator. *Mitigation and Adaptation Strategies for Global Change* **25**, 713–731 (2020).

21. D. P. Keller, *et al.*, The Carbon Dioxide Removal Model Intercomparison Project (CDRMIP): rationale and experimental protocol for CMIP6. *Geosci. Model Dev.* **11**, 1133–1160 (2018).

22. J. G. John, C. A. Stock, J. P. Dunne, A more productive, but different, ocean after mitigation. *Geophys. Res. Lett.* **42**, 9836–9845 (2015).

23. A. H. MacDougall, Reversing climate warming by artificial atmospheric carbon-dioxide removal: Can a Holocene-like climate be restored? *Geophys. Res. Lett.* **40**, 5480–5485 (2013).

24. J. Y. Lee, *et al.*, "Future Global Climate: Scenario-Based Projections and Near-Term Information Supplementary Material" in *Climate Change 2021: The Physical Science Basis. Contribution of Working Group I to the Sixth Assessment Report of the Intergovernmental Panel on Climate Change*, V. Masson-Delmotte, *et al.*, Eds. (2021) https:/doi.org/10.1017/9781009157896.006.

25. K. Zickfeld, D. Azevedo, S. Mathesius, H. D. Matthews, Asymmetry in the climate–carbon cycle response to positive and negative CO2 emissions. *Nat. Clim. Chang.* **11**, 613–617 (2021).

26. G. Danabasoglu, *et al.*, The Community Earth System Model Version 2 (CESM2). *J. Adv. Model. Earth Syst.* **12**, 106 (2020).

27. C. J. Smith, *et al.*, FAIR v1.3: a simple emissions-based impulse response and carbon cycle model. *Geosci. Model Dev.* **11**, 2273–2297 (2018).

28. R. J. Millar, Z. R. Nicholls, P. Friedlingstein, M. R. Allen, A modified impulse-response representation of the global near-surface air temperature and atmospheric concentration

response to carbon dioxide emissions. *Atmos. Chem. Phys.* **17**, 7213–7228 (2017).

29. S. K. Liddicoat, *et al.*, Compatible Fossil Fuel CO2 emissions in the CMIP6 Earth System Models' Historical and Shared Socioeconomic Pathway experiments of the 21st Century. *J. Clim.*, 1–72 (2020).

30. K. Zickfeld, T. Herrington, The time lag between a carbon dioxide emission and maximum warming increases with the size of the emission. *Environ. Res. Lett.* **10**, 031001 (2015).

31. K. Anderson, G. Peters, The trouble with negative emissions. *Science* **354**, 182–183 (2016).

32. P. Smith, *et al.*, Biophysical and economic limits to negative CO2 emissions. *Nat. Clim. Chang.* **6**, 42–50 (2015).

33. S. Fuss, *et al.*, Negative emissions—Part 2: Costs, potentials and side effects. *Environ. Res. Lett.* **13**, 063002 (2018).

34. S. V. Hanssen, *et al.*, Global implications of crop-based bioenergy with carbon capture and storage for terrestrial vertebrate biodiversity. *Glob. Change Biol. Bioenergy* **14**, 307–321 (2022).

35. C. D. Jones, *et al.*, Simulating the Earth system response to negative emissions. *Environ. Res. Lett.* **11**, 095012 (2016).

36. F. Joos, *et al.*, Carbon dioxide and climate impulse response functions for the computation of greenhouse gas metrics: a multi-model analysis. *Atmos. Chem. Phys.* **13**, 2793–2825 (2013).

37. Community Earth System Model developers, CMIP6 CESM2 esm-piControl experiment with CAM6, interactive land (CLM5), coupled ocean (POP2) with biogeochemistry (MARBL), interactive sea ice (CICE5.1), non-evolving land ice (CISM2.1), and CO2 concentration calculated (2019) (June 29, 2022).

38. C. Proistosescu, P. J. Huybers, Slow climate mode reconciles historical and model-based estimates of climate sensitivity. *Sci Adv* **3**, e1602821 (2017).

39. M. A. A. Rugenstein, K. C. Armour, Three flavors of radiative feedbacks and their implications for estimating equilibrium climate sensitivity. *Geophys. Res. Lett.* **48** (2021).

40. K. Caldeira, N. P. Myhrvold, Projections of the pace of warming following an abrupt increase in atmospheric carbon dioxide concentration. *Environ. Res. Lett.* **8**, 034039 (2013).

41. D. W. J. Thompson, E. A. Barnes, C. Deser, W. E. Foust, A. S. Phillips, Quantifying the Role of Internal Climate Variability in Future Climate Trends. *J. Clim.* **28**, 6443–6456 (2015).

42. A. H. MacDougall, The Transient Response to Cumulative CO2 Emissions: a Review. *Current Climate Change Reports* **2**, 39–47 (2016).

Supplementary Information

To understand why the response of CO_2 concentrations in the atmosphere lead emissions in response to an emissions reversal, we can consider a general case of a sinusoidal emissions timeseries, that drives a combined land and ocean sink timeseries that is proportional to emissions but with an additional lag term. We can thus consider the airborne CO_2 change as the sum of two sinusoidal functions, for emissions and sinks respectively, and use the trigonometric identity for addition with arbitrary lags:

$$a\,sin(x\ +\ \theta_A)\ +\ b\,sin\,(x\ +\ \theta_B)\ =c\,sin\,(x\ +\ \varphi)$$

Whose solution terms c (amplitude) and φ (lag) are:

$$c^2\ =a^2\ +\ b^2\ +\ 2\,a\,b\,cos(\theta_A-\theta_B)$$

$$tan(\varphi)=\frac{a\,sin(\theta_A)\ +\ b\,sin(\theta_B)}{a\,cos(\theta_A)\ +\ b\,cos(\theta_B)}$$

In the case of the Earth system response to emissions, the sink magnitude *b* is approximately half of the emissions *a* (i.e. the airborne fraction is roughly ~0.5) and with a lag relative to emissions that is small relative to the timescale of emissions reversal. Thus if we set *a = 1, b = -0.5,* θ_A= 0, and use the small-angle approximation for θ_B, then we can calculate the amplitude c and lag φ of the resulting sum as:

$$c^2\ =1.25\ -\ cos(-\theta_B)$$

$$c\ \approx 0.5$$

And

$$tan(\varphi)=\frac{-0.5\ sin(\theta_B)}{1\ -\ 0.5\,cos(\theta_B)}$$

$$tan(\varphi)\approx\frac{-0.5\,\theta_B}{1\ -\ 0.5}$$

$$\varphi\approx\ -\theta_B$$

Thus we should expect the change in atmospheric CO_2 to have roughly half the amplitude of emissions and lead the emissions by approximately the amount that the sink lags emissions, as is found in CESM2 here.

Supplementary Figures

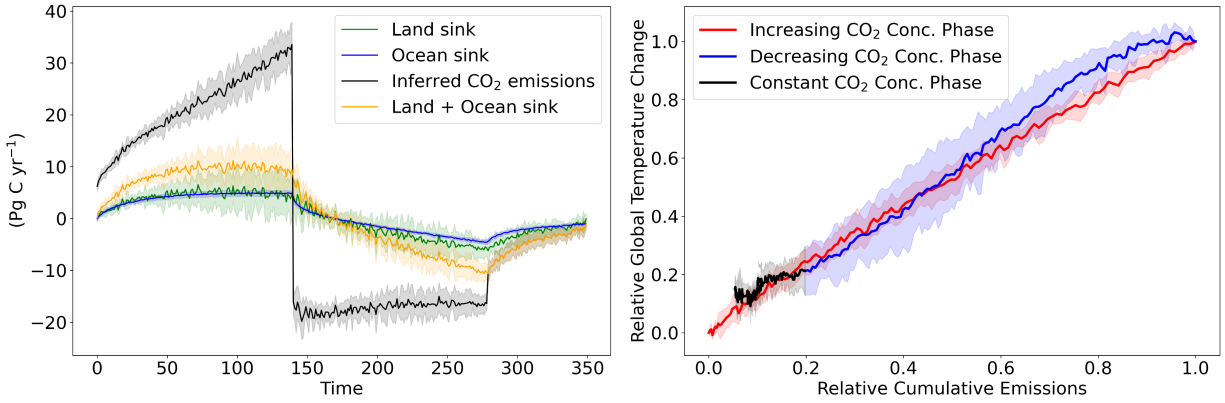

(a) (b)

Fig. S1 (a) Timeseries of land (green), ocean (blue), and combined sink (orange) fluxes, and inferred CO_2 emissions (black), for CMIP6 CDRMIP 1%/yr CO_2 concentration reversal experiment, and (b) T vs CE plot for CMIP6 1%/yr CO_2 concentration reversal CDRMIP experiment (red is for increasing CO_2 concentrations phase, blue is decreasing CO_2 concentrations phase, black is for constant CO_2 concentration phase). Solid lines are ensemble mean and shading is +/- 1σ across ensemble. 7 Earth system models used under the CDRMIP 1%/yr forcing experiment (21): CESM2 (26), CanESM5 (43), CNRM-ESM2-1(44), UKESM1-0-LL (45), ACCESS-ESM1.5 (46), GFDL-ESM4(47), and NorESM2-LM(48). For all models, compatible emissions were calculated based on the sum of land carbon fluxes, ocean carbon fluxes, and atmospheric CO_2, assuming a constant conversion value of 1 ppm CO_2 = 2.124 Pg C(49) for all models. Data available at: CESM2: (50), CanESM5: (51), CNRM-ESM2-1: (52), UKESM1-0-LL: (53), ACCESS-ESM1.5: (54), GFDL-ESM4: (55), and NorESM2-LM: (56).

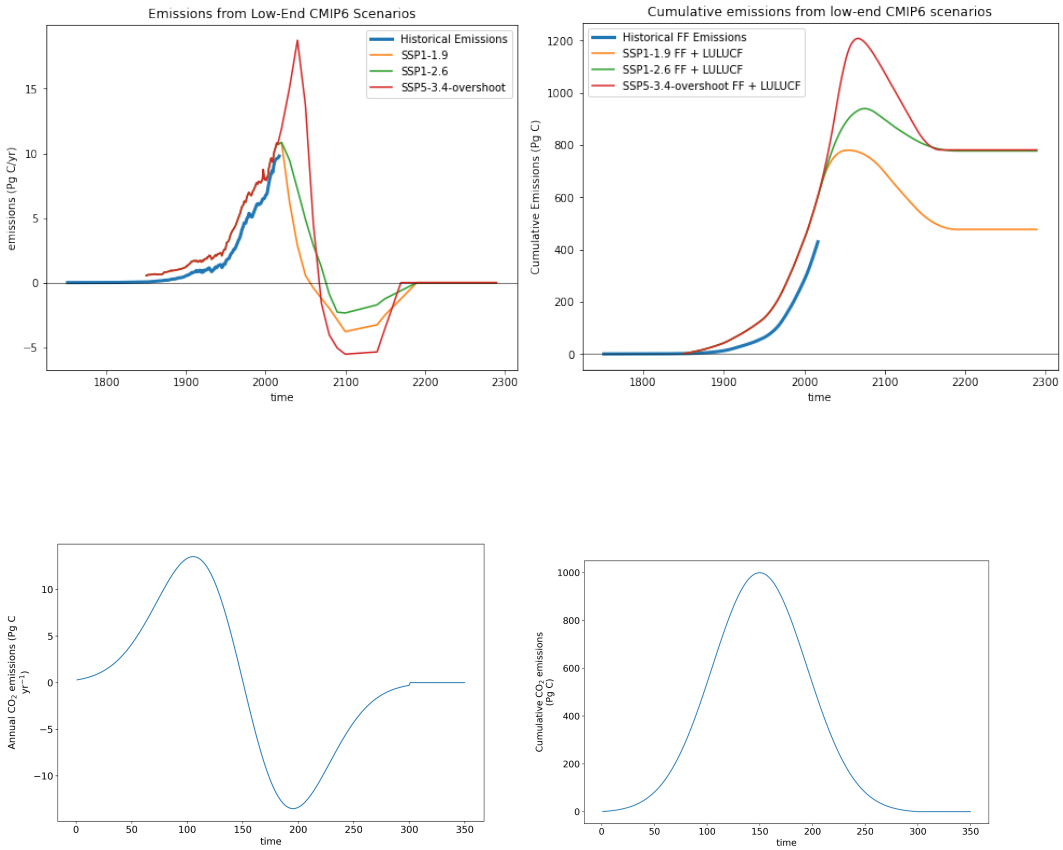

Fig. S2 (a) CO_2 emissions timeseries and (b) cumulative CO_2 emissions timeseries for SSP overshoot scenarios (c) CO_2 emissions timeseries and (d) cumulative CO_2 emissions timeseries for idealized scenario explored here.

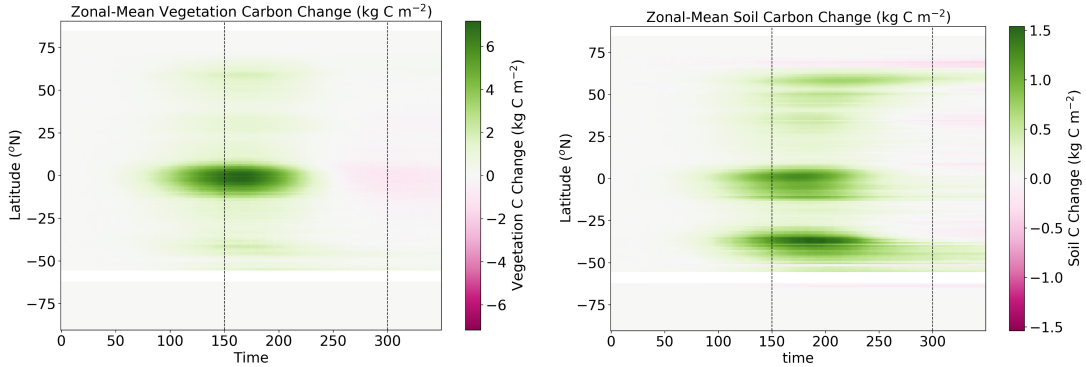

Fig. S3 Zonal-mean trajectories of (a) vegetation and (b) soil carbon change for CESM2 simulation.

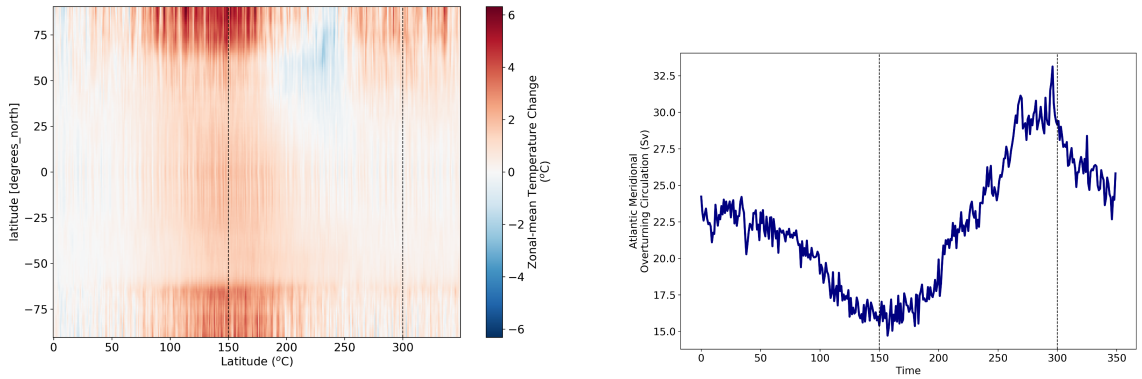

Fig. S4 (a) CESM2 Zonal-mean surface temperature anomalies, and (b) Atlantic meridional overturning circulation through the scenario.

Parameter	Shape parameter	Scale parameter	5th Percentile	50th Percentile	95th Percentile
τ_0	0.6	10^6	3.6e5	1e6	2.6e6
τ_1	0.6	400	140	390	990
τ_2	0.6	100	37	100	260
τ_3	0.6	5	1.8	4.9	1.3

Table S1: Carbon sink timescale parameters (years) for lognormal distributions used in FaIR simple model ensemble.

Parameter	Shape parameter	Scale parameter	5th Percentile	50th Percentile	95th Percentile
q_0	0.6	.5	.20	.50	1.3
q_1	0.6	.33	.13	.33	.41
q_2	0.6	.41	.14	.41	1.1

Table S2: Thermal sensitivity parameters in $KW^{-1}m^2$ for lognormal distributions used in FaIR simple model ensemble.

Parameter	Shape parameter	Scale parameter	5th Percentile	50th Percentile	95th Percentile
d_0	0.6	3000	1100	3100	8200
d_1	0.6	200	70	190	520
d_2	0.6	4	1.5	4.1	10

Table S3: Thermal timescale parameters in years for lognormal distributions used in FaIR simple model ensemble.

Supplementary Information References

43. N. C. Swart, *et al.*, The Canadian Earth System Model version 5 (CanESM5.0.3). *Geoscientific Model Development* **12**, 4823–4873 (2019).

44. R. Séférian, *et al.*, Evaluation of CNRM earth system model, CNRM-ESM2-1: Role of earth system processes in present-day and future climate. *J. Adv. Model. Earth Syst.* **11**, 4182–4227 (2019).

45. A. A. Sellar, *et al.*, UKESM1: Description and Evaluation of the U.K. Earth System Model. *J. Adv. Model. Earth Syst.* **11**, 4513–4558 (2019).

46. T. Ziehn, *et al.*, The Australian Earth System Model: ACCESS-ESM1.5. *J. South. Hemisph. Earth Syst. Sci.* **70**, 193 (2020).

47. J. P. Dunne, *et al.*, The GFDL earth system model version 4.1 (GFDL-ESM 4.1): Overall coupled model description and simulation characteristics. *J. Adv. Model. Earth Syst.* **12** (2020).

48. Ø. Seland, *et al.*, Overview of the Norwegian Earth System Model (NorESM2) and key climate response of CMIP6 DECK, historical, and scenario simulations. *Geosci. Model Dev.* **13**, 6165–6200 (2020).

49. A. P. Ballantyne, C. B. Alden, J. B. Miller, P. P. Tans, J. W. C. White, Increase in observed net carbon dioxide uptake by land and oceans during the past 50 years. *Nature* **488**, 70–72 (2012).

50. G. Danabasoglu, NCAR CESM2 model output prepared for CMIP6 CDRMIP 1pctCO2-cdr (2019) https:/doi.org/10.22033/ESGF/CMIP6.7500.

51. N. C. Swart, *et al.*, CCCma CanESM5 model output prepared for CMIP6 CDRMIP 1pctCO2-cdr (2019) https:/doi.org/10.22033/ESGF/CMIP6.10223.

52. R. Seferian, CNRM-CERFACS CNRM-ESM2-1 model output prepared for CMIP6 CDRMIP 1pctCO2-cdr (2021) https:/doi.org/10.22033/ESGF/CMIP6.9581.

53. C. Jones, S. Liddicoat, A. Wiltshire, MOHC UKESM1.0-LL model output prepared for CMIP6 CDRMIP 1pctCO2-cdr (2020) https:/doi.org/10.22033/ESGF/CMIP6.12183.

54. T. Ziehn, *et al.*, CSIRO ACCESS-ESM1.5 model output prepared for CMIP6 CDRMIP 1pctCO2-cdr (2019) https:/doi.org/10.22033/ESGF/CMIP6.4233.

55. J. G. John, *et al.*, NOAA-GFDL GFDL-ESM4 model output prepared for CMIP6 CDRMIP 1pctCO2-cdr (2018) https:/doi.org/10.22033/ESGF/CMIP6.8476.

56. J. Tjiputra, *et al.*, NCC NorESM2-LM model output prepared for CMIP6 CDRMIP 1pctCO2-cdr (2019) https:/doi.org/10.22033/ESGF/CMIP6.13725.